JVSTB Journal of Vacuum Science & Technology B

Optical property improvement of InAs/GaAs quantum dots grown by hydrogen-plasma-assisted molecular beam epitaxy

A. V. Katkov, C. C. Wang, J. Y. Chi, C. Cheng, and A. K. Gutakovskii

Citation: Journal of Vacuum Science & Technology B **29**, 03C127 (2011); doi: 10.1116/1.3570870
View online: http://dx.doi.org/10.1116/1.3570870
View Table of Contents: http://scitation.aip.org/content/avs/journal/jvstb/29/3?ver=pdfcov
Published by the AVS: Science & Technology of Materials, Interfaces, and Processing

Optical property improvement of InAs/GaAs quantum dots grown by hydrogen-plasma-assisted molecular beam epitaxy

A. V. Katkov[a)]
Department of Engineering and System Science, National Tsing-Hua University, Hsinchu, Taiwan 30013, Republic of China and Taiwan International Graduation Program, Nano-Science and Technology Program, Institute of Physics, Academia Sinica, Taipei 115, Taiwan, Republic of China

C. C. Wang
Mechanical and System Research Laboratories, Industrial Technology and Research Institute, Hsinchu, Taiwan 31040, Republic of China

J. Y. Chi[b)]
Institute of Electronic Engineering, National Dong-Hua University, Hualien, Taiwan 97401, Republic of China

C. Cheng
Department of Electronics Engineering, National Chiao Tung University, Hsinchu, Taiwan 30010, Republic of China

A. K. Gutakovskii
Institute of Semiconductor Physics, Academy of Sciences of Russia, Siberian Division, Novosibirsk 630090, Russia

(Received 28 October 2010; accepted 6 March 2011; published 28 March 2011)

An order-of-magnitude increase of photoluminescence (PL) efficiency at room temperature has been observed in the GaAs/InAs quantum dots (QDs)-in-a-well structure grown with *in situ* irradiation of atomic hydrogen supplied by a radio-frequency hydrogen-plasma source. The enhancement in PL intensity rapidly increases with the hydrogen flow rate and is stable with a variation of excitation power in the radio-frequency plasma source. Extensive thermal annealing of grown samples up to 634 °C did not show any significant degradation of photoluminescence intensity compared with the reference sample. The reduction of nonradiative recombination centers in the as-grown sample causes the greatly enhanced luminescence property. In addition to PL enhancement the authors observed that the H-assisted growth of InAs QDs has suppressed bimodal distribution of QD shape. In contrast to the hydrogen-plasma-assisted growth, irradiation by hydrogen in molecular form has a detrimental effect on the optical properties of similar structures. The high thermal stability of improved optical properties suggests that the formation of the defects which are responsible for nonradiative recombination channels is suppressed during H-assisted epitaxy although *in situ* defect passivation by atomic hydrogen cannot be completely ruled out. © *2011 American Vacuum Society.* [DOI: 10.1116/1.3570870]

I. INTRODUCTION

The major challenges for the heteroepitaxial growth are to minimize the crystalline defects that to hold back many promising device applications. Numerous techniques have been developed to minimize defects during epitaxial growth and/or to anneal them out after growth. Since the presence of defects is inevitable, particularly for the low temperature or lattice mismatched growths, the passivation of defects is also an effective means to neutralize their deleterious effects on device performances. Hydrogen-plasma-assisted molecular beam epitaxy (HA-MBE) has been reported for the epitaxial growth of GaAs based bulk and quantum well materials,[1–3] GaAs on Si(001) substrate,[4] and recently quantum dot (QD) structures.[5,6] H-assisted growth has been used to eliminate the lateral composition modulation during the deposition of the InGaAsP active region for laser structures.[3] It is also reported that the continuous irradiation by atomic hydrogen during epitaxial growth is more efficient for passivation of misfit dislocations than the postgrowth H-plasma treatment.[7] In most of the cases, thermal cracking of molecular hydrogen on a hot tungsten filament is used to provide the atomic hydrogen flux.[1–7] Application of the radio-frequency atomic hydrogen source for HA-MBE is much less studied although some promising results have been demonstrated on InAs transport properties[8] and GaSb/InAs infrared photodiode performance.[9] To improve optical quality by suppressing the formation of nonradiative centers in the GaAs barrier layer grown at low temperature and the highly strained InAs wetting layer[10,11] we focus on the use of the rf plasma source for HA-MBE of the Stranski–Krastanov (SK) growth of InAs QDs on GaAs(001) substrate. Exactly the same QD-in-a-well structure has been grown with different exposure conditions to hydrogen plasma. Order-of-magnitude enhancement in the PL efficiency has been observed for the as-grown samples.

[a)]Electronic mail: andrei.katkov@gmail.com
[b)]Electronic mail: chij@mail.ndhu.edu.tw

TABLE I. Selected published data and results obtained in this work on conditions of oxide desorption from GaAs(001) surface.

T desorption (°C)	Time of oxide desorption (min)	Type of atomic hydrogen source (cracker temperature) (°C)	Reference
400	20	H cracker (not indicated)	1
400	30	H cracker (1900)	14
400	5	H cracker (1500)	15
250	2–5	rf UNI-Bulb; 2 SCCM; 400 W	This work

Furthermore, the thermal stability of the improvement has been tested and found to remain stable up to 634 °C post-growth annealing in an ultrahigh vacuum (UHV). This thermal stability is much higher than that generally observed for *ex situ* hydrogen-plasma treatment,[12,13] suggesting that different passivation mechanisms may be in effect.

II. EXPERIMENT

The epitaxial growth and plasma irradiation for the present work have been done with a semiproduction Riber Epineat system equipped with all solid sources. A Veeco UNI-Bulb rf plasma source is used to provide the atomic hydrogen flux. High purity (5 N) hydrogen gas has been supplied through two millipore molecular filters and a flow rate controller to the rf plasma cell. The hydrogen flux was generated with the plasma source operated in the high brightness mode at excitation frequency of 13.56 MHz. Excitation power varied from 200 to 500 W with typically zero reflected power. An aperture plate containing 150 holes with 0.2 mm in diameter has been used for all experiments described in this work. The plasma source has been opened from the time of oxide desorption at 250 °C to the time after growth when substrate temperature again reached 250 °C. In most of the cases it took from 2 to 5 min for the oxide to desorb with a hydrogen flow rate of 2 SCCM (SCCM denotes cubic centimeter per minute at STP) and rf source excitation power of 400 W. The thermal desorption is performed with no protective As flux which shows the high efficiency of oxide desorption with rf source compared with other existing approaches.[1,14,15] Oxide desorption was confirmed by the appearance of a sharp and streaky (2×1) reflection high-energy electron diffraction (RHEED) pattern. At this moment, we are not able to measure the hydrogen dissociation rate for rf plasma hydrogen source; however, its high efficiency can be indirectly confirmed by a relatively low desorption temperature and a rather short time to obtain the clean GaAs(001) surface during oxide desorption. Some of the published results, including our observations on H-induced oxide desorption from GaAs(001) substrates, are summarized in Table I. After the oxide desorption, the substrate was heated up to 600 °C for growth with a ramp rate of 15 °C/min. The original (2×1) reconstruction gradually changed to the As-stable $c(4\times4)$ as the substrate temperature raised to 450 °C under the As flux. The transition of

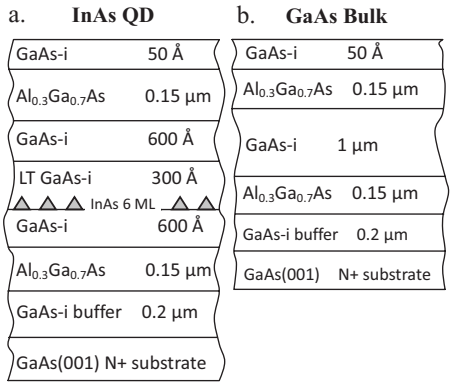

FIG. 1. Schematic illustration of grown structures: (a) a single GaAs/InAs QD layer; (b) a 1 μm GaAs layer is embedded in $Al_{0.3}Ga_{0.7}As$ cladding layers.

RHEED pattern from As-rich $c(4\times4)$ to As-stable (2×4) typically took place at about 540 °C. The bright and streaky RHEED pattern corresponding to As-stable (2×4) surface reconstruction remained clear and sharp until the GaAs buffer layer growth began at 600 °C. No degradation of As-stable (2×4) RHEED pattern at 600 °C was observed after a 1.5 h of exposure to the hydrogen plasma generated with 400 W of rf power and 4 SCCM of hydrogen flow rate.

Two types of structures have been grown by HA-MBE to study the effect of hydrogen flow rate and rf excitation power on their optical properties. The cross section of each type of grown structures and parameters of the rf atomic hydrogen source during growth are summarized in Fig. 1 and Table II, respectively. Self-assembled InAs QDs have been grown in the SK mode at 500 °C at a growth rate equal to 0.011 ML/s under As_4 flux of about 2.0×10^{-6} Torr. All the other layers have been grown at 600 °C under the As-rich conditions with the growth rates of 1 μm/h for GaAs and 1.43 μm/h for AlGaAs. This growth condition was optimized for the long wavelength emission with a narrow peak for QDs. Base pressure during H-assisted growth was about 2.7

TABLE II. Parameters of rf H-plasma cell used in this work.

Run No.	Plasma cell parameters	Structure
84	Without H plasma	InAs QD
85	2 SCCM; 400 W	InAs QD
86	4 SCCM; 400 W	InAs QD
91	Without H plasma	GaAs bulk
92	4 SCCM; 400 W	GaAs bulk
93	8 SCCM; 400 W	GaAs bulk
94	6 SCCM; 400 W	InAs QD
95	8 SCCM; 400 W	InAs QD
96	10 SCCM; 400 W	InAs QD
97	2 SCCM; 300 W	InAs QD
98	2 SCCM; 400 W	InAs QD
99	2 SCCM; 500 W	InAs QD
100	Without hydrogen	InAs QD
101	2 SCCM; molecular hydrogen	InAs QD
102	4 SCCM; molecular hydrogen	InAs QD

$\times 10^{-6}$ Torr for 2 SCCM of hydrogen flow rate and increased up to 1.4×10^{-5} Torr with the increase of hydrogen flow rate up to 10 SCCM. The PL technique has been used to evaluate optical quality. The PL excitation source is the 488 nm line of an argon-ion laser focused on a spot of about 400 μm in diameter and detected by the InGaAs photodiode. Excitation laser power for PL was fixed at 1 mW. A reference sample was used to calibrate the measured PL intensity. All the PL intensity was normalized to this sample to allow comparison of all the intensity measurements. The accuracy of the measurement data is within 10%.

Samples 84, 85, and 86 were isochronally annealed for a 1 h duration in UHV. During annealing, the sample surface has been covered by another piece of GaAs for protection from the thermal decomposition. The temperature of the annealing was measured with a thermocouple calibrated by the melting points of In, Sn, Al–Si alloy, and Al. The accuracy of the temperature measurement was estimated to be within ± 5 °C. All three samples, 84, 85, and 86, were annealed simultaneously. After each anneal, PL spectra were taken at the room temperature (RT) with 1 mW excitation power of Ar^+ laser.

The size and density of the QDs were studied by means of the transmission electron microscopy (TEM) using a JEOL-4000EX (Japan) microscope operated at 400 keV. This microscope is equipped with the improved objective lens pole piece UHP-40H with Cs=0.85 mm and characterized by "point-to-point" resolution of 0.16 nm. The thin foils for TEM investigations were prepared by the routine techniques including grinding and chemical etching.

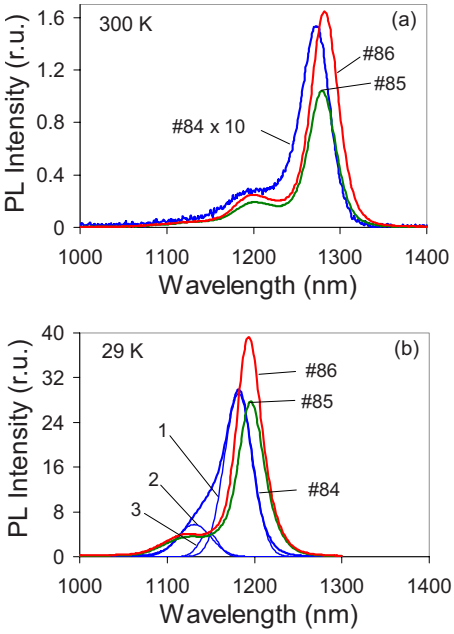

FIG. 2. (Color online) (a) Room temperature PL of three samples with peak wavelength grown at different hydrogen flow rates: 0, 2, and 4 SCCM for 84, 85, and 86, respectively. (b) Low-temperature PL with Gaussian deconvolution of spectral line corresponding to sample 84. The ground state, the excited state, and the ground of additional family of QDs are labeled 1, 2, and 3, respectively.

III. RESULTS AND DISCUSSION

A. Effect of rf source parameters on PL properties

The parameters examined in this work include the hydrogen gas flow rate and power of the plasma source. The effects of the molecular hydrogen and the postgrowth annealing under the plasma are also examined.

The effect of the hydrogen flow rate on the PL property is shown in Fig. 2 which shows the results of the RT and low-temperature PL measurements of the as-grown samples. It can be seen that at room temperature the samples grown under the hydrogen plasma (85 and 86) show one order of magnitude increase from the reference sample (84) with no hydrogen exposure. The greatly enhanced PL intensity indicates the improved crystalline quality. For each spectrum shown in Fig. 2(a), two PL peaks are observed corresponding to the ground state and excited state of the QDs. The ground state peak wavelength for the three spectra is around 1.28 μm and the full width at half maximum of the main peaks is less than 30 meV. These three samples show almost identical spectra except for the intensity, indicating that similar QDs are grown under the hydrogen plasma. However, at low temperature, the enhancement of the PL intensity is greatly reduced as seen in Fig. 2(b) which shows that the three samples have comparable intensity. The peaks of the three samples are blueshifted with respect to those at room temperature by about 70 meV, which is very close to what is expected from the Varshni formula. The shape of the spectra shows some difference with the excited-state peak for the reference sample becoming less separated from the ground state when compared to its room temperature spectrum and to the spectra for the other two samples grown with hydrogen-plasma exposure. An attempt was made to understand the possible reasons for this difference by deconvolution of the spectra with multiple Gaussian peaks. Spectra of sample 84 deconvolute to two-Gaussian peaks with a smaller separation of excited state to ground energy than that at room temperature. Since this is somewhat unreasonable, a three-Gaussian deconvolution was used and the result is shown in Fig. 2(b). Since the TEM observations shown in Fig. 6(b) reveal the existence of bimodal distribution of QDs, the three-Gaussian peaks labeled 1, 2, and 3 can be attributed to, respectively, the ground state, the first excited state, and the ground state of an additional QD family with smaller size than the main family. At high temperature carriers in smaller dots with shallow energy depths from the barrier will have enough thermal energy to escape from these shallow QDs. The escaped carriers will be captured by large QDs[16] and recombined radiatively or will recombine through the nonradiative recombination centers before they are captured. The extra peak is thus absent in the room temperature PL spectra [see Fig. 2(a)]. This analysis and the TEM results are consistent with the assumption that the hydrogen-plasma exposure may prevent the formation of the additional family of smaller QDs during growth.

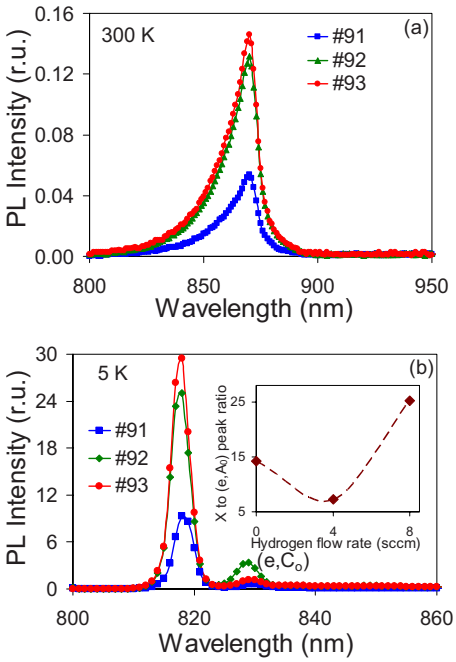

FIG. 3. (Color online) (a) PL of bulk GaAs structure taken at (a) room temperature and (b) 5 K. Ratio of exciton related peak to (*e*, °C) which is caused by carbon incorporation is shown in the inset.

Similar observations on the reduced enhancement of low-temperature PL intensity have also been made by other research groups[12,13] using *ex situ* hydrogen-plasma irradiation of InAs QD samples. Qualitatively it has been explained by the rapid radiative recombination of excited carriers in QDs at low temperature, so possible improvement of the surrounding material by hydrogen passivation cannot be revealed by the PL technique. However, at higher temperatures thermally excited carriers are able to diffuse in the wetting layer and cladding layers. Since the density of nonradiative recombination centers is reduced due to the atomic hydrogen treatment, less carriers are lost to the nonradative recombination centers to allow more carriers to be trapped by the QDs and recombined radiatively to cause the increased PL intensity. This explanation is partially supported by the observation of more than a doubled enhancement of room temperature PL intensity with the use of HA-MBE from GaAs bulk structure shown in Fig. 3(a). Low-temperature PL spectra obtained from these samples provide useful information as well [see Fig. 3(b)]. In addition to the enhancement of bound exciton related peak (*X*) we observed that the transition caused by the carbon incorporation is also enhanced at the 4 SCCM flow rate, but it is significantly suppressed with the increase of the hydrogen flow rate up to 8 SCCM. The ratio of bound exciton peak to the (*e*, C_o) peak with hydrogen flow rate is shown in the inset of Fig. 3(b). We can explain this behavior qualitatively by the insufficient concentration of atomic hydrogen on the surface at a low hydrogen flow rate of 4 SCCM. Increasing the hydrogen flow rate to 8 SCCM enhances atomic hydrogen concentration sufficiently to eliminate the carbon atoms from the surface by the formation and desorption of CH_n volatile compounds.[17]

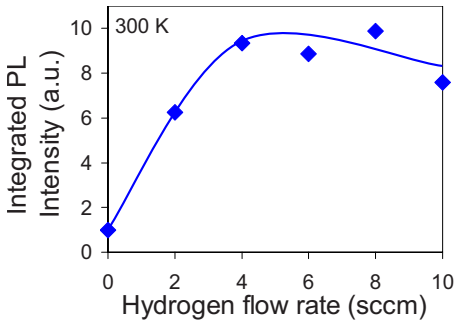

FIG. 4. (Color online) Dependence of integrated PL intensity from hydrogen flow rate at fixed excitation rf power of 400 W.

Dependence of the integrated PL intensity on the hydrogen flow rate with the fixed rf excitation power is shown in Fig. 4. The integrated PL intensity from the QDs saturates quickly and remains stable with an increasing hydrogen flow rate up to 10 SCCM. The rf excitation power was kept constant at 400 W for each flow rate with the exception of the 10 SCCM case. In that case, the rf excitation power has to be increase up to 500 W in order to keep the hydrogen plasma in high brightness mode.

The effects of molecular hydrogen on the room and low-temperature PL properties of the InAs based QD structure are shown in Figs. 5(a) and 5(b), respectively. The degradation of room temperature PL may be qualitatively explained by the higher concentration of carbon in the InAs QD layer from exposure to molecular hydrogen, which has CO_2 and CO contents in the ppm level. It has been reported that carbon incorporation is attributed to the generation of nonradiative

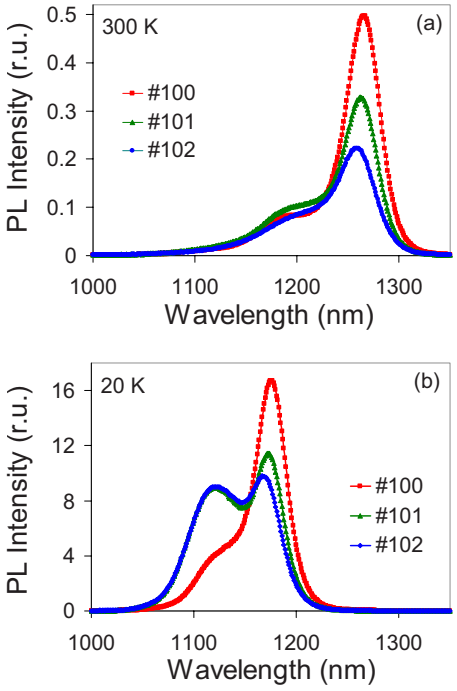

FIG. 5. (Color online) Effect of irradiation by molecular hydrogen on (a) room temperature and (b) low-temperature PLs from InAs QD based structure.

centers in InAs material.[18] The low-temperature spectra shown in Fig. 5(b) have two peaks which correspond to the ground states of two different InAs QD families. The intensity of the high-energy peak, corresponding to the smaller QD size family, increases with the flow rate of the molecular hydrogen. The appearance of the smaller size QD family can be tentatively explained by the carbon induced faceting of InAs surface in the same way as it was reported for GaAs.[19]

The density of QDs corresponding to three different growth conditions was calculated from the plane view TEM images shown in Fig. 6. For the case of the hydrogen-plasma-assisted growth (sample 98) shown in Fig. 6(a), we found that the QD density is 6.2×10^9 cm^{-2}. Two types of QD shapes can be found on the images shown in Figs. 6(b) and 6(c) corresponding to the H-free case (sample 100) and the case grown under molecular hydrogen flow (sample 102), respectively. One family of QDs has an oval shape which also appears in the hydrogen-plasma-assisted growth shown in Fig. 6(a), and the other has the pyramidal shape which does not appear in samples with hydrogen-plasma-assisted growth. In the case of H-free growth (sample 100), QD densities of oval and pyramidal shapes were equal to 8×10^9 and 1×10^9 cm^{-2}, respectively. For the samples grown with 2 SCCM of molecular hydrogen, the densities of oval and pyramidal dots were equal to 4×10^9 and 2×10^9 cm^{-2}, respectively. Pyramidal shape QDs have been never observed in the samples grown by HA-MBE. Plane view TEM observations confirm the PL indications of the existence of bimodal distribution of QDs for the samples grown without hydrogen and especially for samples grown with molecular hydrogen.

To see the effects of *postgrowth* exposure using the present plasma source and conditions, some samples were exposed to the hydrogen plasma after growth. Different pieces cut from sample 84 have been put back into the vacuum chamber and exposed to hydrogen plasma with the identical plasma conditions as used in sample 86 for 5 and 60 min at two different temperatures of 250 and 450 °C. After the plasma treatment, the samples were measured again. No change in the room temperature PL spectrum was observed. This observation indicates that the PL enhancement in the case of HA-MBE is caused exclusively by the *in situ* H-assisted growth and not due to the plasma exposure during the cooling down cycle of the sample when the plasma source was kept on. This is different from the published results where PL intensity from similar InAs based QD structures has been observed to increase after the *ex situ* irradiation by atomic hydrogen.[12,13] This difference can be explained by the order higher hydrogen concentration which was used for postgrowth treatment,[12] while this kind of plasma source is not compatible with typical MBE technique.

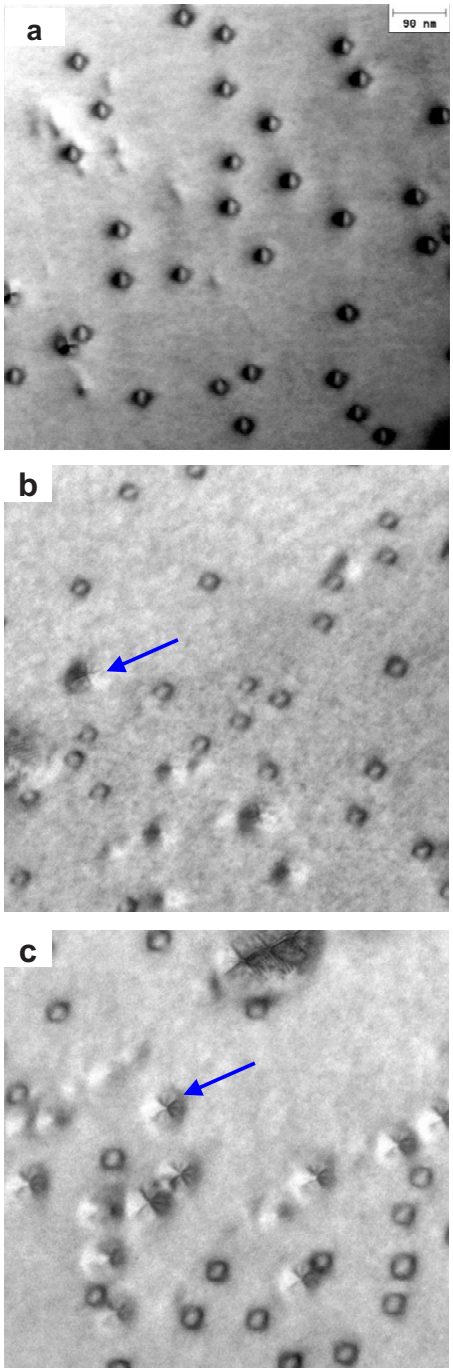

FIG. 6. (Color online) Plane view TEM images: (a) 98, rf cell: 2 SCCM, 400 W; (b) 100, hydrogen free. Pyramidal shape QD is indicated by an arrow: (c) 102, 2 SCCM of molecular hydrogen. Pyramidal shape QD is indicated by an arrow.

B. Thermal stability

Previous works using *ex situ* hydrogen passivation have shown that the effect of hydrogen-plasma treatment is thermally unstable, and the improved PL intensity largely disappeared above 300 °C due to the outdiffusion of hydrogen after the thermal treatment.[12,13] Since thermal stability of enhanced performance is important for practical application due to the required annealing steps during device processing, the present samples are subjected to a 1 h isochronal annealing at various temperatures in UHV conditions. All three samples—84, 85, and 86—were annealed simultaneously. After annealing, PL was taken at room temperature with 1 mW excitation power. The integrated PL intensities of samples 85 and 86 along with the reference sample 84 after

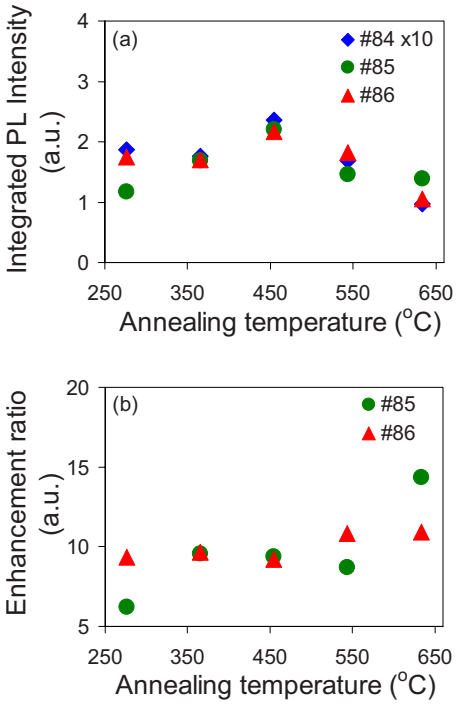

FIG. 7. (Color online) (a) Variation of integrated PL intensity with annealing temperature. (b) Enhancement ratio as a function of annealing temperature. Annealing time was kept for 1 h at each temperature.

each annealing are shown in Fig. 7(a) as a function of annealing temperature. Improvement of optical properties attributed to H-plasma-assisted growth can be characterized by the enhancement ratio which is equal to the ratio of integrated PL intensity from the sample grown by H-assisted epitaxy to the integrated PL intensity from H-free sample. The variation of the enhancement ratio for samples 85 and 86 with annealing temperature is shown in Fig. 7(b). It can be seen that the enhancement of PL intensity for samples grown under hydrogen plasma is maintained up to the final annealing temperature of 634 °C, slightly below the congruent sublimation temperature. The peak wavelength and the FWHM after each annealing are also shown in Fig. 8. Only a slight blueshift in wavelength about 5 nm is seen from all three samples. The FWHMs, however, remain roughly unchanged. Small decrease of integrated PL intensity observed after 450 °C in Fig. 7(a) and the small blueshift of the peak wavelength shown in Fig. 8 could be caused by In outdiffusion from QDs, which leads to lower carrier confinement although surface degradation during annealing may also play a role. Further study is required to clarify the mechanism. This stability after thermal annealing of the QD samples grown under H-plasma irradiation is remarkable and is very different from other reports with *ex situ* H-plasma treatment. For example, a 5 min annealing at 600 °C (Ref. 13) or for 1 h at 400 °C (Ref. 12) has been shown to completely eliminate the passivation effect. In the present case of HA-MBE with radio-frequency hydrogen-plasma source, however, no decrease in enhancement ratio (ratio of integrated PL intensity from a sample grown by HA-MBE to the integrated PL intensity of the control sample 84) with annealing temperature has been observed up to 634 °C. Since the passivation of the defects by atomic hydrogen tends to be annealed out at this temperature, it is possible that the absence of this annealing-out effect indicates that the reduced incorporation of defects during growth may be responsible for optical improvement for this work rather than passivation of their effect.

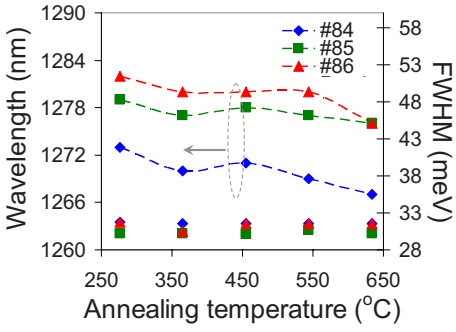

FIG. 8. (Color online) Peak wavelength and FWHM as a function of annealing temperature.

IV. SUMMARY AND CONCLUSIONS

In summary, we have demonstrated some beneficial effects of hydrogen assisted MBE with a rf hydrogen-plasma source. Room temperature PL intensity is about one order higher than the conventional hydrogen free case. This improvement in PL properties is stable with extensive temperature annealing, which cannot be achieved with any *ex situ* hydrogen treatment. The suppression of nonradiative recombination centers during growth is the main cause for PL enhancement. Transition from bimodal growth mode of InAs QDs for the conventional H-free case or under the molecular hydrogen flux to one family growth mode was observed with HA-MBE.

ACKNOWLEDGMENT

The authors gratefully acknowledge the support of the National Science Council of the Republic of China under Contract No. NSC 97-2218-E-259-002-MY3.

[1]Y. Okada, T. Sugaya, S. Ohta, T. Fujita, and M. Kawabe, Jpn. J. Appl. Phys., Part 1 **34**, 238 (1995).
[2]K.-Y. Jang, Y. Okada, and M. Kawabe, J. Cryst. Growth **206**, 267 (1999).
[3]R. R. LaPierre, D. A. Thompson, and B. J. Robinson, Semicond. Sci. Technol. **13**, 637 (1998).
[4]Y. Okada, H. Shimomura, and M. Kawabe, J. Appl. Phys. **73**, 7376 (1993).
[5]Y. J. Chun, S. Nakajima, Y. Okada, and M. Kawabe, Physica B **227**, 299 (1996).
[6]R. Oshima and Y. Okada, Thin Solid Films **464–465**, 229 (2004).
[7]M. Yokozeki, H. Yonezu, T. Tsuji, and N. Ohshima, J. Cryst. Growth **175–176**, 435 (1997).
[8]Y. Q. Chen, T. Unuvar, D. Mscicka, and W. I. Wang, J. Vac. Sci. Technol. B **24**, 1599 (2006).
[9]Y. Chen, A. Moy, S. Xin, K. Mi, and P. P. Chow, Infrared Phys. Technol. **52**, 340 (2009).
[10]T. Asano, Z. Fang, and A. Madhukar, J. Appl. Phys. **107**, 073111 (2010).
[11]S. W. Lin, C. Balocco, M. Missous, A. R. Peaker, and A. M. Song, Phys. Rev. B **72**, 165302 (2005).

[12]Q. X. Zhao, A. P. Jacob, M. Willander, S. M. Wang, Y. Q. Wei, F. Ferdos, M. Sadeghi, A. Larssonb, and J. H. Yang, Phys. Lett. A **315**, 150 (2003).
[13]E. C. Le Ru, P. D. Siverns, and R. Murray, Appl. Phys. Lett. **77**, 2446 (2000).
[14]H. Nagano, Z. Qin, A. Jia, Y. Kato, M. Kobayashi, A. Yoshikawa, and K. Takahashi, J. Cryst. Growth **189–190**, 265 (1998).
[15]T. Sugaya and M. Kawabe, Jpn. J. Appl. Phys., Part 2 **30**, L402 (1991).
[16]L. Brusaferri *et al.*, Appl. Phys. Lett. **69**, 3354 (1996).
[17]S. Goto, Y. Nomura, Y. Morishita, Y. Katayama, and H. Ohno, Jpn. J. Appl. Phys., Part 1 **33**, 3825 (1994).
[18]Z. M. Fang, K. Y. Ma, R. M. Cohen, and G. B. Stringfellow, Appl. Phys. Lett. **59**, 1446 (1991).
[19]G. Laurence, F. Simondet, and P. Saget, Appl. Phys. (Berlin) **19**, 63 (1979).